Shifts in diversification rates linked to biogeographic movement into new areas: an example of a recent radiation in the Andes[1]

Simon Uribe-Convers[2] and David C. Tank

Department of Biological Sciences, University of Idaho, 875 Perimeter MS 3051

Moscow, ID, 83844–3051, USA

[1]Manuscript received _____; revision accepted _____.

[2]Author for correspondence: Simon Uribe-Convers; email: uribe.convers@gmail.com, web: www.simonuribe.com

Acknowledgements

We would like to thank S. Mathews for kindly sharing genomic DNA for some taxa used in this study. J. Sullivan, L. Harmon, E. Roalson, J. Beaulieu, B. Moore, N. Nürk, M. Pennell and XX anonymous reviewers for helpful suggestions or comments on the manuscript. J. Beaulieu, L. Harmon, C. Blair and the University of Idaho Institute for Bioinformatics and Evolutionary Studies (NIH/NCRR P20RR16448 and P20RR016454) for computational aid. Funding for this work was provided by NSF DEB–1210895 to DCT for SUC, NSF DEB–1253463 to DCT, and Graduate Student Research Grants to SUC from the Botanical Society of America (BSA), the Society of Systematic Biologists (SSB), the American Society of Plant Taxonomists (ASPT), and the University of Idaho Stillinger Herbarium Expedition Funds.

47 *Premise of the study*: Clade specific bursts in diversification are often associated with the
48 evolution of key innovations. However, in groups with no obvious morphological innovations,
49 observed upticks in diversification rates have also been attributed to the colonization of a new
50 geographic environment. In this study, we explore the systematics, diversification dynamics, and
51 historical biogeography of the plant clade Rhinantheae in the Orobanchaceae, with a special
52 focus on the Andean clade of the genus *Bartsia* L..

53 *Methods*: We sampled taxa from every major lineage of Rhinantheae, as well as a representative
54 sample of Andean *Bartsia* species. Using standard phylogenetic methods, we reconstructed
55 evolutionary relationships, inferred divergence times among the major lineages of Rhinantheae,
56 elucidated their biogeographic history, and investigated diversification dynamics.

57 *Key results*: We confirmed that the South American *Bartsia* species form a highly supported
58 monophyletic group. Rhinantheae was estimated to have a median crown age of ca. 30 Ma, and
59 Europe played an important role in the biogeographic history of the lineages. South America was
60 first reconstructed in the biogeographic analyses around 9 Ma, and with a median age of 2.59
61 Ma, this clade shows a significant uptick in diversification.

62 *Conclusions*: Increased net diversification of the South American clade corresponds with
63 biogeographic movement into the New World. This happened at a time when the Andes were
64 reaching the necessary elevation to host an alpine environment. Although a certain route of
65 dispersal to South America cannot be described, we provide plausible hypotheses to how the
66 group colonized the New World.

67 Keywords**:** *Bartsia*; *Bellardia*; Dispersification; Neobartsia; Orobanchaceae; Páramo;

68 Rhinantheae

69

70

71

72

73

74

75

76

77

78

79

80

81

82

83

84

85

86

87

88

The investigation of global patterns of biodiversity has a long history (e.g., Mittelbach et al., 2007). With the increase in our knowledge of phylogenetic relationships as well as methods for using phylogenies to understand diversification rates and biogeographic patterns (e.g., Ree et al., 2005; Alfaro et al., 2009), these global patterns can now be placed in an explicitly historical context (sensu Moore and Donoghue, 2007). Along these lines, differences in species richness between geographic areas have often been explained by climatic stability, age of the region, and/or niche conservatism that contributes to the slow, but steady, accumulation of species over time (Wiens and Donoghue, 2004). Likewise, clade specific bursts in net diversification (speciation minus extinction) are often associated with the evolution of novel morphologies, referred to as key innovations, such as nectar spurs in angiosperms (e.g., Hodges, 1997), molar characters in mammals (Woodburne et al., 2003), and feathers in birds (Ostrom, 1979). More recently, Moore and Donoghue (2007) demonstrated that in the plant families Adoxaceae and Valerianaceae, shifts in diversification rates were not correlated with the evolution of novel floral characters, but rather, with the movement into new geographic areas, and hypothesized that "dispersification" (dispersal and diversification) may play a larger role in shaping global biodiversity patterns than previously recognized. This is equivalent to the "key opportunity" of Donoghue and Sanderson (2015), and follows the hypothesis that in newly emerging environments, as long as the corridors for biogeographic movements are in place, these new areas will often be filled with lineages from environmentally similar areas where the relevant morphological and/or physiological adaptations are already in place (Donoghue, 2008). Empirical tests of these hypotheses not only require a robust estimate of phylogenetic relationships, but also the estimation of divergence times, diversification rates, and biogeographic patterns for the group of interest.

Various approaches have been taken to assess phylogenetic relationships, divergence times, and rates of diversification – each increasing our understanding of biodiversity and the way in which it has been produced. Bayesian analyses are now regularly used to estimate divergence times (e.g., Bacon et al., 2012; Drummond et al., 2012), most often performed in the program BEAST (Drummond and Rambaut, 2007), because the use of probabilistic priors accommodates for both phylogenetic uncertainty (i.e., topology and branch lengths), as well as the timing of calibration points. Diversification rate analyses have been instrumental to our understanding of disparities in clade richnesses across the tree of life. For example, Alfaro et al. (2009) suggested that several pulses of diversification instead of single events have shaped the current diversity of jawed vertebrates. Additionally, in the plant genus *Asclepias* L. (milkweeds) it has been shown that increases in the rate of diversification are tightly associated with the evolution of defense traits that prevent or minimize herbivory, and that this resulted in an adaptive radiation in the group (Agrawal et al., 2009). Finally, studies of Andean plants, e.g., the family Valerianaceae (Bell and Donoghue, 2005b) and the genus *Lupinus* L. (Hughes and Eastwood, 2006; Drummond et al., 2012), have shown that groups with North American temperate ancestors have elevated diversification rates in the Andes, given that they were "pre–adapted" to the conditions of the newly and unoccupied niche at the time that they colonized the Andes.

To investigate the influence of biogeographic movements on rates of diversification, we have chosen to study the mostly European clade Rhinantheae of the parasitic plant family Orobanchaceae (Wolfe et al., 2005; Bennett and Mathews, 2006; McNeal et al., 2013), with a particular focus on the genus *Bellardia* All., a clade of 48 species that are disproportionally distributed across two disjunct geographic regions. The majority of the species in *Bellardia* were

135 formerly part of the genus *Bartsia* L., but it has been recently recircumscribed (Scheunert et al.,
136 2012) to better reflect the evolutionary history of its species. Prior to this taxonomic
137 rearrangement, *Bartsia* (49 spp.) had two species distributed in the mountains of northeastern
138 Africa (*B. decurva* Benth. and *B. longiflora* Benth.), one in the Mediterranean region (*B. trixago*
139 L.), one in Scandinavia, the Alps, Greenland and the Hudson Bay region of northeastern North
140 America (*B. alpina* L.), and the remaining 45 species distributed throughout the páramos of
141 Andean South America (Molau, 1990). Broad–scale phylogenetic studies of Orobanchaceae
142 (Wolfe et al., 2005; Bennett and Mathews, 2006) and the Rhinantheae clade (Těšitel et al., 2010)
143 had suggested that *Bartsia* was not monophyletic, but Scheunert et al. (2012) were the first to
144 include species from the complete geographic distribution of the genus, as well as the two
145 species of the related Mediterranean genus *Parentucellia* Viv.. However, because their sampling
146 only included two species of the South American clade of *Bartsia*, they chose to only reclassify
147 these two species, leaving ca. 43 species in a large polyphyletic group with the monotypic
148 lineage of *B. alpina* in Europe. The South American *Bartsia* species, which we will refer to here
149 as the *Neobartsia* clade, are quite distinct from their Mediterranean counterparts (i.e., *Bellardia*
150 *trixago,* and the two species of *Parentucellia* that were also moved to the expanded genus—
151 *Bellardia latifolia* and *B.* viscosa) in multiple aspects. Ecologically, *Neobartsia* species grow at
152 high elevation (ca. 3,000–5000 m) in wet environments while the Mediterranean species grow at
153 low elevation (ca. 0–500 m) in seasonally dry environments. Geographically, *Neobartsia* is
154 restricted to the Andes while the Mediterranean taxa are native to the Mediterranean region and
155 more recently have been introduced to Australia, coastal Chile, and coastal western North
156 America. Finally, the Mediterranean species all have reflexed corolla lips, usually associated
157 with bee pollination, whereas a large number of the species in *Neobartsia* have erect corolla lips

158 that are thought to be associated with hummingbird pollination due to their tubular shape and the
159 placement of reproductive parts.

160 Previous studies of the group have only included a minor fraction of the South American
161 species richness, usually sampling only one or two species, making it difficult to assess the
162 influence of biogeographic movements on rates of diversification across the clade. Here, we
163 included representatives from all of the major lineages comprising the former genus *Bartsia,*
164 including a morphologically and geographically representative sampling of the South American
165 diversity, as well as a representative sampling of all known allied genera of the Rhinantheae
166 clade of Orobanchaceae, to establish a robust and well–supported phylogeny of the clade based
167 on both chloroplast and nuclear ribosomal DNA sequence data. We then use this phylogeny to
168 estimate divergence times across the clade and to investigate the biogeographic history of the
169 clade, with a special focus on the origin of the *Neobartsia* clade in Andean South America.
170 Finally, we use all these analyses to test if increases in rates of diversification are indeed
171 associated with biogeographic movements into newly formed environments, i.e.,
172 "dispersification" sensu Moore and Donoghue (2007).

173

174 ## MATERIALS AND METHODS

175 ***Sampling—***

176 A total of 49 taxa were included in this study (Table 1), with newly collected specimens
177 stored in airtight plastic bags filled silica gel desiccant in the field. Because our main focus is the
178 diversification dynamics of the South American *Neobartsia* clade in the context of the disparate
179 geographic distributions of the Old World species and the remainder of the mostly European
180 Rhinantheae clade of Orobanchaceae, our sampling effort included representatives of 10 of the

11 genera thought to comprise the clade (Wolfe et al., 2005; Bennett and Mathews, 2006; Těšitel et al., 2010; Scheunert et al., 2012; McNeal et al., 2013). *Bellardia* and the *Neobartsia* clade are represented here by 15 South American species and two of the three Mediterranean taxa, *Bellardia trixago* (L.) All. and *Bellardia viscosa* (L.) Fisch. & C.A. Mey. The South American species were selected as to encompass the morphological and geographic diversity in the clade. Based on previous results (Olmstead et al., 2001; Wolfe et al., 2005; Bennett and Mathews, 2006; Těšitel et al., 2010; Scheunert et al., 2012; McNeal et al., 2013) *Melampyrum* L. was used as the outgroup for the Rhinantheae clade.

Molecular Methods—

Total genomic DNA was extracted from silica gel–dried tissue or herbarium material using a modified 2X CTAB method (Doyle and Doyle, 1987). Two chloroplast (cp) regions–*trnT–trnF* region and the *rps16* intron–were amplified via polymerase chain reaction (PCR) using the *trn*–a and *trn*–f (Taberlet et al., 1991) and the *rps16*_F and *rps16*_R primers (Oxelman et al., 1997), respectively. The nuclear ribosomal (nr) internal transcribed spacer (ITS) and external transcribed spacer (ETS) regions were amplified using the ITS4 and ITS5 primers (Baldwin, 1992) and the ETS–B (Beardsley and Olmstead, 2002) and 18S–IGS (Baldwin and Markos, 1998), respectively. PCR profiles for all regions followed Tank and Olmstead (2008). When amplification of a region in one fragment was not possible, internal primers were used to amplify the region in multiple fragments. The primer pairs *trn–a/trnb, trnc/trn–d,* and *trn–e/trn–f* (Taberlet et al., 1991) were used to amplify the *trnT–trnF* region. Additionally, *Bellardia* specific internal primers were designed and used when these primer combinations failed (*trnT/trnL* intergenic spacer: *trnT–L_iF* 5–CTTGGTTTTCATCCGTAAAGG–3 and *trnT–L_iR*

204 5–CCTTTACGGATGAAAACCAAG–3). Following Tank and Olmstead (2008), the
205 *rps16*_F/*rps16*_iR and *rps16*_iF/*rps16*_2R primer combinations were used to amplify the *rps16*
206 intron in two fragments. Similarly, the ITS5/ITS2 and ITS3/ITS4 primer combinations (Baldwin,
207 1992) were used to amplify the ITS region in two fragments.
208 PCR products were purified by precipitation in a 20% polyethylene glycol 8000
209 (PEG)/2.5 M NaCl solution and washed in 70% ethanol prior to sequencing. To ensure accuracy,
210 we sequenced both strands of the cleaned PCR products on an ABI 3130xl capillary DNA
211 sequencer (Applied Biosystems, Foster City, California, USA) using ABI BigDye v.3.1 cycle
212 sequencing chemistry. Sequence data were edited and assembled for each region using the
213 program Sequencher v.4.7 (Gene Codes Corp., Ann Arbor, Michigan, USA), and consensus
214 sequences were generated and submitted to GenBank (GenBank accessions: ETS: KM408174–
215 KM408207, ITS: KM408208–KM408238, *trnT–trnL*: KM408239–KM408278, *rps16*:
216 KM408279–KM408316, *trnL–trnF*: KM434082–KM434123). When sequencing was not
217 possible for any given species or gene region, GenBank sequences were used to reduce the
218 amount of missing data in the final matrix (Table 1).
219
220 ***Phylogenetic Analyses—***
221 Although two separate cpDNA regions were sequenced, the evolutionary histories of the
222 *trnT–trnF* region and the *rps16* intron are tightly linked due to the nonrecombining nature of the
223 chloroplast genome, and thus, were treated as a single locus. The nrDNA regions (ITS and ETS)
224 were also treated as a single locus, given that they are linked because of their physical proximity
225 in the nrDNA repeat. We created three primary datasets with our two independent loci: 1)
226 cpDNA only, 2) nrDNA only, and 3) a combined cpDNA and nrDNA dataset. Global alignments
227 across the Rhinantheae clade were created for each gene region using the group–to–group profile

228 alignment method as implemented in Muscle v.3.6 (Edgar, 2004). This method takes advantage
229 of previous knowledge about monophyly of the major lineages (e.g., Těšitel et al., 2010;
230 Scheunert et al., 2012) and consists of lineage–specific alignments that are then iteratively
231 aligned to one another resulting in fewer alignment ambiguities (Smith et al., 2009). These
232 alignments were visually inspected and minor adjustments were made manually using Se–Al
233 v.2.0a11 (Rambaut, 1996). Sites that could not be unambiguously aligned were excluded from
234 the analyses. File format conversions and matrix concatenations were performed using the
235 program Phyutility v.2.2 (Smith and Dunn, 2008).
236 A statistical selection of the best–fit model of nucleotide substitution according to the
237 Akaike information criterion (AIC) was conducted independently for each gene region using the
238 program jModelTest (Guindon and Gascuel, 2003; Posada, 2008). Based on these results,
239 partitioned (by gene region) maximum likelihood (ML) analyses were performed on our three
240 primary datasets using RAxML v. 7.2.4 (Stamatakis, 2006) with 1,000 replicates of
241 nonparametric bootstrapping using the rapid bootstrap algorithm (Stamatakis et al., 2008). Every
242 fifth bootstrap tree generated by the rapid bootstrap analyses was used as a starting tree for full
243 ML searches and the trees with the highest ML scores were chosen. Likewise, partitioned
244 Bayesian inference (BI) analyses were performed using the parallel version of MrBayes v3.1.2
245 (Ronquist and Huelsenbeck, 2003) with the individual parameters unlinked across the data
246 partitions. Analyses consisted of two independent runs with four Markov chains using default
247 priors and heating values. Each independent run consisted of 15 million generations and was
248 started from a randomly generated tree and was sampled every 1,000 generations. Convergence
249 of the chains was determined by analyzing the plots of all parameters and the –lnL using Tracer
250 v.1.5 (Rambaut and Drummond, 2004). Stationarity was assumed when all parameters values

and the –lnL had stabilized; the likelihoods of independent runs were considered indistinguishable when the average standard deviation of split frequencies was < 0.001. Consensus trees were obtained for each dataset using the sumt command in MrBayes. Finally, incongruencies between the cpDNA and the nrDNA topologies were investigated using the approximately unbiased (AU) test (Shimodaira, 2002) and the Shimodaira–Hasegawa (SH) test (Shimodaira and Hasegawa, 1999), as implemented in the program CONSEL (Shimodaira and Hasegawa, 2001).

Divergence Time Estimation—

To maximize the number of taxa and minimize the amount of missing data in our dating analyses, we reduced our combined dataset to include sequences for only the cpDNA *trnT–trnL* intergenic spacer and the nrDNA ITS region. This resulted in a dataset that included all 49 taxa and only 2% missing data, compared to 15% missing data for the complete dataset. Each gene was treated as a separate partition. To ensure convergence in divergence times, five independent runs were conducted using BEAST v.1.5.4 (Drummond and Rambaut, 2007). BEAST implements Markov Chain Monte Carlo (MCMC) methods that allow for uncertainty in both the topology and the calibration points, i.e., calibration points are treated as probabilistic priors, rather than point estimates (Ho and Phillips, 2009). It also implements an uncorrelated lognormal relaxed clock (UCLN) (Drummond et al., 2006), allowing every branch to have an independent substitution rate.

Each run was started from the resulting ML tree obtained for the dataset containing all regions, after performing a semiparametric rate smoothing based on penalized likelihood (Sanderson, 2002) in R (R Development Core Team, 2013) using the package Ape (Paradis et

al., 2004). Each run consisted of 100,000,000 generations sampled every 1000 trees. The models of nucleotide substitution were kept unlinked for both partitions and the tree priors were kept as default under the birth–death process.

Because of the mostly herbaceous habit of the species in Orobanchaceae, there are no known fossils for the family. This lack of fossils made the dating of our analyses dependent on secondary calibrations obtained from a previous study. Based on age estimates of an ITS molecular clock (Wolfe et al., 2005), a calibration point at the node containing every genus except *Melampyrum* (i.e*.,* one node higher than the root) was used. This was done with a lognormal distribution prior with an offset of 25 million years (Ma), a mean of 0.9, and a standard deviation of 0.8, this way incorporating uncertainty in the calibration point. Because the use of this secondary calibration is far from ideal, to corroborate our calibration strategy, an additional analysis using the most recent uplift of the Andes as the calibration point (Simpson, 1975; Burnham and Graham, 1999; Gregory-Wodzicki, 2000; Antonelli et al., 2009) was conducted with a lognormal distribution prior (offset of 1.7 Myr, a mean of 0.2 and an standard deviation of 0.6). This calibration prior was set at the node where the species in *Neobartsia* diverge from *B. viscosa*. This additional calibration scenario was conducted to assess the impact of alternative calibration points in the node ages.

Convergence of the parameters was monitored using Tracer v. 1.5 and the resulting trees were summarized using TreeAnnotator v.1.5.4 (Drummond and Rambaut, 2007) after 25% of the trees had been discarded as burn–in. Each of the five topologies and their node heights were visualized using FigTree v. 1.3.1 (Rambaut, 2006) and a final tree, representing the maximum clade credibility tree with information of the 95 percent highest posterior density (HPD), was obtained by combining the five runs using LogCombiner v.1.5.4 (Drummond and Rambaut,

297 2007) and by summarizing them with TreeAnnotator v.1.5.4.

298

299 ***Biogeographic Analyses—***

300 The biogeographic history of *Bellardia* and allied genera was reconstructed using the
301 program Lagrange v. C++ (Ree and Smith, 2008). Lagrange implements the Dispersal–
302 Extinction–Cladogenesis (DEC) model (Ree et al., 2005) to estimate the most likely ancestral
303 geographic range based on current distributions of extant lineages. This model assumes
304 extinction or dispersal by contraction or expansion of the ancestral geographic range,
305 respectively. Additionally, the user is given the option to assign a dispersal probabilities matrix
306 based on prior knowledge of connectivity between areas, incorporating valuable ancestral
307 geographic information. However, most of this knowledge, at least for Northern Hemisphere
308 temperate plants, is based on macrofossils of woody mesophytic taxa, e.g., *Quercus* (Tiffney and
309 Manchester, 2001). Because the herbaceous genus *Bellardia* is almost completely restricted to
310 alpine–like conditions, which separates this lineage from the ecological conditions in which
311 mesophytic forest species are found, and the vast majority of the Rhinantheae clade is also
312 herbaceous, we consider that biological routes for these types of taxa are less well understood
313 (Donoghue and Smith, 2004). Therefore, we did not include a dispersal probability matrix in our
314 analyses (see also Smith and Donoghue, 2010).

315 We used Lagrange on a posterior distribution of 1,000 randomly chosen trees (post burn–
316 in) from our dating analyses. By inferring ancestral ranges over a posterior distribution of trees
317 we are incorporating uncertainty in both topology as well as times of divergence (Smith, 2009;
318 Smith and Donoghue, 2010; Beaulieu et al., 2013). We conducted three independent analyses
319 with varying distributions of current taxa. The first analysis was performed with conservative

geographic ranges following Mabberley's Plant–Book (Mabberley, 2008), in which the genera have wider distributions, e.g,. the genus *Euphrasia* L. has a north temperate distribution (Eurasia, Europe and Eastern North America). The second analysis included prior expert knowledge about the distribution of the genera based on published work, e.g., we followed the proposed Eurasian origin for the genus *Euphrasia* (Gussarova et al., 2008). The final analysis was based on species–specific distributions based on the explicit species that we sampled, i.e., species within a genus can have different distributions to account for endemisms and/or disparate distributions within a genus.

We considered species to be distributed in five distinct geographic areas: i) Eurasia (western Eurasia: the Balkan Peninsula and the Caucasus region), ii) Europe (including the Mediterranean climatic region in southern Europe and northern Africa), iii) Africa (montane northeastern Africa), iv) North America (Hudson Bay region of northeastern North America), and v) South America (including only the Andes). The results of the analyses were summarized in R. Following Beaulieu et al. (2013), we calculated Akaike weights for every biogeographic scenario reconstructed at every node in each tree separately. We then summed the Akaike weights for each node and averaged them across the distribution of trees, which resulted in composite Akaike weights (w_i) for our biogeographic reconstructions. Furthermore, we examined the evidence for the most supported scenario by calculating an evidence ratio of this model versus all models (Burnham and Anderson, 2002). These were interpreted as relative evidence of one scenario being the most supported when comparing it with competing biogeographic hypotheses (Beaulieu et al., 2013).

343 ***Diversification Rates—***

344 Diversification rates analyses were conducted on the same posterior distribution of 1,000
345 trees, as well as on the maximum clade credibility (MCC) tree using MEDUSA (Alfaro et al.,
346 2009), which is an extension of the method described by Rabosky et al. (2007) and is available in
347 the R package geiger 2.0 (Pennell et al., 2014). In Rabosky et al. (2007), two likelihoods are
348 estimated for a dated tree: i) a phylogenetic likelihood that uses the timing of the splits on the
349 backbone to estimate ML values for birth and death rates following the equations of Nee et al.
350 (1994), and ii) a taxonomic likelihood that uses species richness along with the date of the splits,
351 estimating diversification rates following Magallón and Sanderson (2001). MEDUSA (Alfaro et
352 al., 2009) looks for shifts in diversification rates in a stepwise manner by comparing AIC scores
353 of successively more complex models. This method requires complete sampling that is achieved
354 by collapsing every clade to a single tip and then assigning clade richnesses to these tip lineages.
355 We collapsed our trees into tips representing each of the major lineages of Rhinantheae, which in
356 most cases corresponds to each of the genera. The following clade richnesses were used:
357 *Neobartsia* clade (45 spp.), *Parentucellia* clade (2 spp.), *Bellardia* clade (1 sp.), *Odontites* clade
358 (32 spp.), *Euphrasia* clade (350 spp.), *Rhinanthus* clade (45 spp.), *Melampyrum* clade (35 spp.),
359 *Lathraea* clade (7 spp.), *Rhynchocorys orientalis* (1 spp.), *Rhynchocorys elephas* (1 spp.),
360 *Rhynchocorys odontophylla* (1 spp.), *Rhynchocorys kurdica* (1 spp.), *Rhynchocorys stricta* (1
361 spp.), *Rhynchocorys maxima* (1 spp.), *Bartsia alpina* (1 spp.), *Tozzia alpina* (1 spp.), *Hedbergia*
362 *abyssinica* (1 spp.), *Hedbergia decurva* (1 spp.), *Hedbergia longiflora* (1 spp.).

363 To compare our MEDUSA results we conducted an additional analysis using the program
364 SymmeTREE v1.0 (Chan and Moore, 2005). SymmeTREE is based on the topological
365 distribution of species on the whole tree, which is compared to a distribution simulated on a tree

366 under the equal–rates Markov random branching model (EMR), where the probability of a
367 branching event is constant throughout the tree (Yule, 1924). If a clade shows an unbalanced
368 distribution of species richness when compared to its sister clade, then a shift in the rate of
369 diversification is identified. SymmeTREE also estimates several whole tree statistics that are
370 evaluated against their own simulated null distribution, i.e., a constant pure–birth model (Chan
371 and Moore, 2005). To accommodate topological and temporal uncertainty, we assessed
372 diversification rate shifts with SymmeTREE using default settings across a random set of 542
373 trees from the posterior distribution of trees from our divergence time analysis; the full set of
374 1,000 trees was not used due to computational limitations.
375
376 RESULTS
377 ***Molecular Methods—***
378 The cpDNA data set included the *trnT–trnF* region and the *rps16* intron and had a total
379 length of 2,686 bp with 13% missing data (Table 1). Similarly, the nrDNA dataset included the
380 ITS and ETS regions with a total of 1,134 bp and 17% missing data (Table 1). A combined data
381 set was created from the cpDNA and the nrDNA matrices, with a total length of 3,820 bp and
382 15% missing data (files deposited in the Dryad Digital Repository: *data will be submitted after*
383 *acceptance of the manuscript*).
384
385 ***Phylogenetic Analyses—***
386 Alignment of individual gene regions was straightforward requiring minor adjustments to
387 the automated alignment strategy implemented in MUSCLE v. 3.6 (matrices and trees are
388 available on TreeBase: *Temporary reviewer access*

389 http://purl.org/phylo/treebase/phylows/study/TB2:S11528?x–access–
390 code=334b76effd95e3f56eb4ffe0185fc9ad&format=html). Some regions that could not be
391 unambiguously aligned in the *trnT–trnL* intergenic spacer and in the ETS region were excluded
392 from the analyses (*trnT–L*: alignment positions 519–529 and 587–620; ETS: alignment positions
393 63–65, 83–85 and 152–158). Model selection for the cpDNA regions yielded the General Time
394 Reversible model + Γ (GTR) (Rodríguez et al., 1990) for the *trnT–trnF* intergenic spacer, and the
395 Transversion model + Γ (TVM) for the *rps16* intron. The ITS and ETS regions resulted in the
396 selection of the GTR+I+Γ and Hasegawa–Kishino–Yano+ Γ (HKY) models, respectively. To
397 avoid the difficulties of estimating Γ and the invariable sites simultaneously (Ronquist and
398 Huelsenbeck, 2003; Yang, 2006), the model of substitution GTR+Γ with an increase in the
399 number of rate categories from four to six was preferred in the case of the ITS region.
400 Our results from every dataset (Fig. 1 for the combined dataset and Fig. 2 for the cpDNA
401 and nrDNA datasets) are in concordance with those presented in previous Rhinantheae studies
402 (Těšitel et al., 2010; Scheunert et al., 2012), and assessment of incongruences between the
403 cpDNA and nrDNA datasets showed that these were either not significant, or if they were, the
404 alternative topology was only weakly supported. For example, the well–supported relationships
405 in the cpDNA dataset between *Tozzia alpina* and *Hedbergia*—or between *Odontites* and
406 *Bellardia*—are not statistically significant when constrained in the nrDNA dataset. Conversely,
407 the relationship between *H. abyssinica* var. *nykiensis* and *H. decurva* found in the cpDNA
408 dataset is significant in the AU Test, but it is only moderately supported on the tree (BS 72, PP
409 0.96) and it does not exist in the combined dataset (Table 2). An important new result from this
410 study, which is based on the first widespread sampling of the group, is that the South American
411 species indeed form a distinct clade, the *Neobartsia* clade, that is very well supported with a

412 posterior probability (PP) of 1.0 and a bootstrap support (BS) of 100. *Bellardia*–including the
413 *Neobartsia* clade–is sister to *Odontites* (PP 1.0, BS 92) and together are sister to a clade
414 comprised by *Hedbergia* and *Tozzia alpina* (PP 1.0, BS 93). The placement of the genus *Tozzia*
415 was uncertain until now, although the support of our analyses is marginal (PP 0.94, BS 80).
416 Finally, the genus *Euphrasia* is sister to the latter genera (PP 1, BS 100) and together form a
417 clade sister to *Bartsia alpina* (PP 1, BS 100). This last clade is what Scheunert et al. (2012)
418 referred to as the core Rhinantheae.
419
420 ***Divergence Time Estimations—***
421 When the calibration point was placed at the node where *Melampyrum* diverged from the
422 remaining genera, the South American *Neobartsia* clade was inferred to have a median age of
423 2.59 Ma (1.51–4.08 Ma 95% HPD) (Table 3). The split between *Bellardia trixago* and the
424 remaining species in the clade was estimated to have a median age of 8.73 Ma (5.12–12.76 Ma).
425 The African clade diverged from *Tozzia alpina* 13.64 Ma (8.78–18.70 Ma), while the split of the
426 European *Bartsia alpina* occurred 22.62 Ma (17.49–28.07 Ma). The root of the tree was
427 estimated to have a median age of 30.65 Ma (25.55–38.83 Ma). Likewise, when the geological
428 constraint was imposed, the *Neobartsia* clade had a median age of 2.63 Ma (1.97–3.58 Ma), and
429 the divergence of *Bellardia trixago* from the remaining *Bellardia–Neobartsia* species occurred
430 8.48 Ma (4.95–12.48 Ma). The African clade diverged from *Tozzia alpina* 13.51 Ma (8.69–18.75
431 Ma), *Bartsia alpina* of 22.33 Ma (16.23–28.36 Ma), and the root of the tree was estimated at
432 30.98 Ma (29.13–35.96 Ma). The age of the root is consistent with the date (35.5 Ma) inferred
433 for this clade in an angiosperm wide analysis (Zanne et al., 2014). Because the results using
434 different calibration strategies were within the 95 percent HPD of each other (see Table 3), we

435 used the root calibration analysis for subsequent biogeographic and diversification rate analyses.

436

437 ***Biogeographic Analyses—***

438 Our three different codings of current geographic distribution resulted in very similar
439 ancestral reconstructions (Table 4). Given that so much work has been done in recent years for
440 several of these groups, e.g., *Bartsia/Bellardia* (Molau, 1990)*, Euphrasia* (Gussarova et al.,
441 2008), and *Odontites* (Bolliger, 1996), we favored the second coding scenario where current
442 distributions were based on expert knowledge, including recent phylogenetic and biogeographic
443 studies (for a wide-scale example on campanulids see Beaulieu et al., 2013). The most recent
444 common ancestor (mrca) of the Rhinantheae clade of Orobanchaceae was likely distributed in
445 Europe with a composite Akaike weight (w_i) of 0.31 and an evidence ratio of 1.82 (Table 2).
446 This ancestral range is maintained throughout the backbone of the tree until the node where
447 *Euphrasia* diverges from the rest of the genera (w_i = 0.43, evidence ratio = 1.95). Nevertheless, a
448 European ancestral range becomes the most supported reconstruction again at the node of
449 divergence of *Odontites* (w_i = 0.80, evidence ratio = 8.88). A South American ancestral range is
450 included for the first time at the crown node of *Bellardia*, where a w_i 0.26 supports a split
451 between Europe and South America and a w_i of 0.18 supports an entirely European ancestral
452 range; the evidence ratio between these two reconstructions is 1.44. The node where the
453 *Neobartsia* clade diverges from the Mediterranean *Bellardia viscosa* is again supported by two
454 competing models i) a split between Europe and South America (w_i = 0.53, evidence ratio = 1.51)
455 and ii) one between South America and an area comprised of Europe and Eurasia (w_i = 0.35).
456 Additional results for other genera can be seen on figure 3 and summarized in Table 4.

457

458

Diversification Rates—

Our analyses discovered six shifts in the rate of net diversification (r = speciation minus extinction) in the Rhinantheae clade when performed over the posterior distribution of trees; three of these were also identified on the MCC tree. Importantly, the three shifts identified on the MCC tree corresponded to the shifts that occurred at the highest frequency in the analyses across the posterior distribution of trees. Because most of these analyses were conducted on a posterior distribution of trees to incorporate phylogenetic uncertainty (both temporal and topological), we report the mean net diversification rate of each shift (r_{mean}) on the text and the ranges of these shifts in Table 5. For the three shifts found in the MCC tree, we also report that value (r_{mcc}). The first two shifts found in our analyses correspond to shifts that were only present in less than 15 percent of the trees and show minimal deviation from the background rate of the tree. One of these shifts is on the node subtending the core Rhinantheae (r_{mean} = 0.11, frequency = 0.07) and the other one involves the hemiparasitic genus *Rhinanthus* L. and the holoparasite *Lathraea* L. (r_{mean} = 0.17, frequency = 0.12). The latter shift could correspond to a change in life history from hemiparasitism to holoparasitism in *Lathraea*, but given the limited sampling of these two groups and the low frequency at which the shift was found we dare not comment further. The next shift involves a slowdown in the rate of *Bartsia alpina* (r_{mean} = –0.4, r_{mcc} = 0) and was the most frequent shift in the analyses (frequency = 1.17). The frequency higher than 1.0 for this node is an artifact of the way MEDUSA adds the shifts. When two sister clades each have a shift at their crown nodes, MEDUSA adds the parameters from both shifts and places the result on the stem leading to the two clades. Thus these shifts do not occur with a frequency higher than 1.0, but are very common. The fourth shift corresponds to an increase in net diversification (r_{mean} = 0.09) in the clade sister to *Bartsia alpina* and was found with a frequency of 0.32. An additional

482 shift was found in the clade comprised of *Tozzia alpina* and the genus *Hedbergia*, the shift was
483 found in 75% of the trees (r_{mean} = 0.06; r_{mcc} = 0.05). Finally, a shift showing an uptick in net
484 diversification rate was present for the *Neobartsia* clade, with a frequency of 0.40 (r_{mean} = 0.40;
485 r_{mcc} = 0.79).

486 In comparison, the results obtained with SymmeTREE evidenced fewer diversification
487 shifts on the whole tree ($p < 0.05$). Like the MEDUSA results, an increase in diversification rate
488 was also leading to the clade sister to *Bartsia alpina* and was consistently found in every tree we
489 analyzed (Table 5). A shift showing a slowdown in the *Tozzia*+*Hedbergia* clade was found to be
490 marginally significant at $p < 0.05$ ($p = 0.067$) in every tree. If we were to choose a less stringent
491 significance threshold (e.g., $p < 0.10$), this shift would be significant in 506 trees (93% of the
492 distribution). The same is true for the shift involving the *Neobartsia* clade, where it was only
493 found to be significant in 77 trees at $p < 0.05$ (14%), but increased to 258 trees (48%) when the
494 less stringent p value was chosen.
495
496 DISCUSSION
497 ***Systematic Implications—***
498 Molau (1990) published a comprehensive monograph on the genus "*Bartsia"*, where he
499 hypothesized that the species formed a monophyletic group that was sister to the African
500 monotypic genus *Hedbergia.* Our phylogenetic results (Figs. 1 and 2), which are in agreement
501 with those of Těšitel et al. (2010) and Scheunert et al. (2012), show clearly that *Bartsia* sensu
502 Molau is polyphyletic, and that the new classification (sensu Scheunert et al., 2012) better
503 reflects the disparate geographic distributions of these lineages, as well as their evolutionary
504 histories. Previous studies have recovered the basal relationships within *Bellardia* as a polytomy

505 (Těšitel et al., 2010; Scheunert et al., 2012), where the position of *B. trixago, B. viscosa*, and *B.*
506 *latifolia* is uncertain. Here, we recovered *Bellardia trixago* as the earliest divergent lineage but
507 because we did not sample *B. latifolia*, we cannot be certain of the position of the other two taxa.
508 The South American *Neobartsia* clade was highly supported in every analysis, and this is the
509 first study to sample a geographically and morphologically representative diversity of the
510 richness in this clade. These results provide strong evidence of the evolutionary distinctiveness
511 of the *Neobartsia* clade with respect to the Mediterranean members of the expanded genus
512 *Bellardia* (sensu Scheunert et al. 2012) – i.e., its unique geographic distribution and
513 biogeographic history, the long divergence times from their Mediterranean relatives (~7.39 Ma),
514 and the elevated diversification rates. Along with diagnostic morphological characters, we feel
515 this justifies a reanalysis of the generic revision of Scheunert et al. (2012) with respect to the
516 taxonomy in this clade, and this is the subject of ongoing taxonomic work in this clade.
517 Our cpDNA and nrDNA analyses placed the genus *Tozzia* in different positions in the
518 tree, although these differences were not statistically significant (Table 2). Our combined
519 analysis placed the genus as sister to *Hedbergia*, albeit with marginal support (PP 0.94, BS 80).
520 While this relationship is in agreement with previous studies (Těšitel et al., 2010; Scheunert et
521 al., 2012), further work will be necessary to confidently place this genus in the Rhinantheae
522 clade. Lastly, the African genus *Hedbergia* showed interesting and likely problematic species
523 delimitations. The taxon *H. abyssinica* var. *nykiensis* was sister to *H. decurva* in our cpDNA
524 analyses, and its relationship to the other *H. abyssinica* varieties in the nrDNA dataset was
525 weakly supported. This is the first time that varietal taxa for this group have been included in a
526 molecular study, and highlights the necessity for a more detailed study on the clade.
527

Biogeography and Diversification Rates—

Our divergence time and biogeographic results depicted in figure 3 illustrate evolutionary hypotheses regarding the current distribution of the Rhinantheae clade. As a reminder, our analyses were calibrated using dates obtained with the molecular rate of the ITS (Wolfe et al., 2005), and thus, they should be taken as estimates where some uncertainty is expected. Nevertheless, they provide an evolutionary foundation that helps explain the current distribution and the diversity of the South American *Neobartsia* clade. With no doubt, Europe played a major role, almost at every node, in the reconstruction of ancestral ranges in the Rhinantheae clade of Orobanchaceae. Although this is the first formal biogeographic analysis in the clade, these results are in line with the verbal biogeographic scenarios described in previous studies (Wolfe et al., 2005; Těšitel et al., 2010), but with slight differences in the description of the ancestral areas. Diversification of the majority of the genera was achieved in the European continent with subsequent migration events to Eurasia, northeastern North America, the Mediterranean region, Africa and South America. *Bartsia alpina* is a good example of a taxon with a purely European ancestral distribution but that is currently distributed in other parts of the world. This suggests that the current distribution was the result of a second and more recent migration into Greenland and northeastern North America sometime along its very long branch (Fig. 3). *Odontites* is another good example of a European radiation that has expanded its range to include Eurasia after the initial divergence. Moreover, the genus *Euphrasia*, which accounts for more than half of the members of the clade with ~400 species, was reconstructed as having a Europe/Eurasian ancestral range. The few species sampled in this study all have Eurasian distributions but the genus is currently considered to have a "bipolar" distribution (Gussarova et al., 2008), with species distributed in north temperate regions and extreme Austral areas. This pattern is

551 extremely interesting since it suggests that extinction and/or long distance dispersal have played
552 a large role in shaping the current distribution of this large clade.

553 The Mediterranean region was not included as a distinct area in our reconstruction
554 analyses, and therefore, some of the genera with current Mediterranean distributions were treated
555 as European, e.g., *Rhynchocorys, Odontites*, *Bellardia trixago*, and *B. viscosa*. The
556 Mediterranean climate, as recognized today, is a young environment formed only 2.3–3.2 Ma
557 and it is the result of two main events: i) the establishment of the Mediterranean rhythm of dry
558 summers and mild–cold winters ~3.2 Ma, and ii) the oldest xeric period know for the region ~2.2
559 Ma (Zagwin, 1960; 1974; Suc, 1984). The crown clades for each of these genera were
560 reconstructed to have a European ancestral distribution, which implies that their current ranges
561 are the results of independent evolutions into the European Mediterranean climatic region not
562 earlier than ~3.2 Ma.

563 This study is mainly focused on studying the disproportionate diversity of the *Neobartsia*
564 clade in the Andes, and to propose plausible hypotheses for its distribution. The Andes are
565 thought to have begun uplifting in the late Miocene (~10 Ma) but only reaching the necessary
566 elevation to host alpine conditions in the late Pliocene or early Pleistocene 2–4 Ma (Simpson,
567 1975; Burnham and Graham, 1999; Gregory-Wodzicki, 2000; Antonelli et al., 2009). In our
568 biogeographic analyses, South America is reconstructed for the first time at the crown node of
569 *Bellardia*, with a median age of 8.73 Ma (5.12-12.76 Ma), and then at the node where *Bellardia*
570 *viscosa* and the *Neobartsia* clade diverge (median age of 7.39 Ma [4.21-11.24 Ma]).
571 These reconstructions, between 12.76 and 4.21 Ma, define an eight and a half million year
572 window for the ancestor to have reached South America. There are two main land routes that
573 were present during this time period, the North Atlantic Land Bridge (NALB) uniting

574 northeastern North America and western Europe, and the Bering Land Bridge between eastern
575 Asia and western North America. Previous studies in the plant family Malpighiaceae (Davis et
576 al., 2002; 2004), have suggested a migration route from South America to Africa starting in the
577 early Oligocene (~30 Ma) via North America, the NALB, and Europe. The NALB was available
578 from the early Eocene (~50 Ma) until the middle to late Miocene (~10–8 Ma) (Tiffney, 1985;
579 Tiffney and Manchester, 2001; Denk et al., 2010; 2011), dates which overlap with our
580 divergence time estimates (Table 3) and with the appearance of South America as an ancestral
581 range in our biogeographic analyses. This allows for the possibility of an early dispersal from
582 Europe into North America over this land bridge. Colonization of North America would have
583 followed a stepwise migration to South America over the forming Isthmus of Panama and/or
584 island chains sometime in the last 4.5 Ma (Coates et al., 2004; Kirby and MacFadden, 2005;
585 Retallack and Kirby, 2007). An alternative stepwise migration scenario for the South American
586 clade's colonization of the Andes involves a migration route through Beringia. This land bridge,
587 which was available on–and–off from ~58–3.5 Ma (Hopkins, 1967; Tiffney and Manchester,
588 2001; Tiffney, 2008), has been proposed as a route for several groups found both in eastern Asia,
589 western north America**,** and the Andes—e.g., Valerianaceae (Moore and Donoghue, 2007)**.** This
590 migration scenario is also plausible since Eurasia, Europe, and South America were
591 reconstructed as the second most supported ancestral range at the node of divergence of the
592 South American clade ($w_i = 0.35$).

593 Both of these stepwise migration scenarios rely completely on North America as an
594 intermediary step where the South American ancestor possibly diversified, migrated, and finally
595 went extinct. Unfortunately, there is no fossil record in the Rhinantheae clade (or in
596 Orobanchaceae), and thus, no physical evidence is available to support either of these

hypotheses.

Molau (1990) hypothesized that the *Neobartsia* clade had colonized the Andes via a long–distance dispersal from Africa, sometime in the early Pliocene (~5 Ma). This hypothesis seemed plausible at the time when no phylogenetic evidence was available for the clade, but now that it is clear that the former genus *Bartsia* is polyphyletic and the two African species (*Hebergia decurva, H. longifolia*) are not sister to the South American species, there is no longer support for this hypothesis. Nevertheless, there is a third hypothesis that does rely on long–distance dispersal, but rather from Mediterranean Europe/north Africa to Andean South America (or, alternatively, from somewhere in North America following a land bridge migration from the Old World). Many plants are dispersed over long distances by water (e.g., *Cocos* L.), birds (e.g., *Pisonia* L.), or wind (e.g., *Taraxacum* F.H. Wigg.), and physiological and morphological adaptations to float, adhere, or fly are common (reviewed in Howe and Smallwood, 1982). The seeds of *Bellarida–Neobartsia* are enclosed in a dry dehiscent capsule that contains between 20–200 small seeds (0.3–2 mm) per fruit, each equipped with 6–13 short wings or ridges (Molau, 1990). Although these seeds are light and have wings making them at first glance suitable for long distance traveling, it has been estimated that their mean dispersal distance is 0.3 meters, at least in *Bartsia alpina* (Molau, 1990). The short mean dispersal distance is in strong disagreement with the distance that a seed would need to travel from the Mediterranean region to the New World (~7,000 km/~4,000 mi). Nevertheless, there is a known constant storm track from western Africa (including the northwestern African Mediterranean climatic region) that crosses the Atlantic Ocean into the Caribbean and the Americas, and recent evidence has shown that there are major influxes of African dust in southern North America (Bozlaker et al., 2013), northeastern South America (Prospero et al., 2014), and the Caribbean basin (Prospero and

620 Mayol-Bracero, 2013). This opens the possibility for seeds of a Mediterranean ancestor to have
621 been picked up and carried over to the New World. Although at first this may seem unlikely, it is
622 important to point out that a single seed may be sufficient for the colonization of a new habitat,
623 and that the eight and a half million year time window coupled with the large amounts (~200) of
624 seeds that are produced in each capsule, increase the probability for this event to have happened.
625 At this point we cannot accept or reject any of the biogeographic hypotheses described
626 above—the two stepwise migrations through North America or the long–distance dispersal from
627 the Mediterranean climatic region—and it highlights the difficulty of inferring ancestral
628 colonization routes even when using modern ancestral range reconstruction methods (see Tripp
629 and McDade, 2014), especially with a non–existent fossil record. Nevertheless it is interesting to
630 study and discuss some of the caveats that these hypotheses have. The route over the NALB
631 requires that the migration from the Old World occurred sometime between 12–8 Ma, which
632 based on palynological evidence (Denk et al., 2010; 2011) is the latest time that this land bridge
633 was available. This timeframe overlaps with the oldest estimates of our dating analyses (5.12-
634 12.76 Ma), but leaves a narrower window of time for a stepwise migration to have occurred.
635 Furthermore, the warmer temperatures in eastern North America during the late Miocene would
636 possibly have affected the migration of a presumably alpine adapted ancestor through the NALB.
637 Conversely, the Bering Land Bridge was available until ~3.5 Ma, which overlaps completely
638 with both the divergence of the South American clade from *Bellardia viscosa* (4.21-11.24 Ma),
639 as well as with the split between *Bellardia trixago* and the other members of the *Bellardia–*
640 *Neobartsia* clade 5.12–12.76 Ma. Moreover, this more recent route allows for the world to cool
641 down during the Pliocene (Tiffney and Manchester, 2001), which may have facilitated the
642 migration. Importantly, with either route, a stepwise migration hypothesis implies that the

643 ancestral lineage (and any of its descendants) would have then gone extinct thereafter in North
644 America and in eastern Asia (if the Bering Land Bridge route is considered).

645 To investigate if these biogeographic movements have affected the rate at which clades
646 are diversifying (i.e., "dispersification"), we need to assess if the shifts found in our analyses
647 correlate with a movement into a new area or if there is something else, e.g., a morphological
648 change, that has triggered them. Regardless of the reason, investigating shifts of diversification
649 and the location of these on a phylogenetic tree is extremely helpful when trying to understand
650 disparities in species richnesses across related clades. The comparison of two methods that are
651 based on different tenets, a stepwise model testing approach vs. a topological imbalance
652 approach (MEDUSA and SymmeTREE, respectively), allowed us to i) better evaluate the
653 performance of different approaches used to identify shifts in diversification, while ii) making
654 results shared by both methods robust and reliable. This comparison also showed the advantages
655 of using a stepwise model testing approach and a method that incorporates extinction. Our
656 MEDUSA analysis found six shifts across the posterior, and three when using the MCC tree; two
657 of these six identified shifts represent a slowdown in net diversification. One of these
658 slowdowns, which is the only shift consistently found by SymmeTREE at $p < 0.01$, across the
659 posterior, and in the MCC tree, corresponds to the node where *Bartsia alpina* diverges from the
660 rest of the core Rhinantheae 22.62 Ma. The extremely low diversification rate and its very long
661 branch indicate that this species is likely the only extant member of a lineage that has had
662 historically very low speciation rates or high extinction rates, or both. The first significant
663 increase in net diversification rates was found at the node where the genus *Euphrasia* diverges
664 from other genera 19.25 Ma. This genus includes ~400 species that encompass more than 80% of
665 the species richness of Rhinantheae, estimated to be ~528 spp. (Mabberley, 2008). Based on our

666 limited sampling of this group, we cannot identify an apparent change in morphology or
667 geography in the genus, and thus, no evident cause for this shift can be assessed with these data.
668 Nevertheless, given the age and very high diversity of the clade, this shift is not surprising.
669 However, it is important to point out that because we collapsed clades at the generic level to
670 incorporate unsampled diversities, the present shift might not be the only one in *Euphrasia* and
671 that clades within the genus may also have shifts of their own, where there might be an apparent
672 change in either morphology or geography.

673 We also identified an increased rate of net diversification in the South American
674 *Neobartsia* clade. We hypothesize that the clade underwent a similar pattern as seen in other
675 Andean radiations, e.g. the family Valerianaceae and the genus *Lupinus* (Bell and Donoghue,
676 2005a; Hughes and Eastwood, 2006, respectively), where their North American ancestor was
677 "pre–adapted" to cold environments making the colonization of the high Andes, and further
678 radiation, easier (Donoghue 2008). The *Neobartsia* clade has a median divergence time of 2.59
679 Ma and a mean diversification rate of 0.40, however, when the analysis is performed on the
680 MCC tree, the net diversification almost doubles (r_{mcc} = 0.79). The large difference in values
681 implies that although the shift was only identified in 40% of the posterior distribution of trees,
682 when detected, the rate can be nearly four times higher than the background rate of the tree
683 (background r_{mean} = 0.22). Based on the very short branches within the clade, its young age, and
684 the genetic similarity between the species included in this study, this shift likely resulted in a
685 rapid radiation event where the movement to and colonization of the high Andes acted as a
686 trigger to increased diversification. As the Andes were uplifting, the creation of new vacant
687 niches and the simulation of alpine conditions promoted the radiation into the diversity that we
688 see today. Accordingly, this is a another example of how phylogenetic niche conservatism and

689 the movement into a new geographic area, can lead to a high number of species in a relatively
690 short period of time without the appearance of morphological key innovation, which is what
691 Moore and Donoghue (2007) referred to as "dispersification".
692
693 ***Conclusions—***
694 This study places the *Neobartsia* clade in the context of a robust and well–supported
695 phylogeny within the Rhinantheae clade of Orobanchaceae. This is the first study to study this
696 clade in an explicitly temporal framework, with detailed divergence time estimates for the clade.
697 Here, we focused primarily on the colonization and diversification of Andean South America
698 ~2.59 Ma. This date correlates well with the necessary age for the Andes to have acquired the
699 adequate elevation to simulate alpine conditions for the establishment of this temperate, largely
700 alpine clade in South America. Given that the South American clade is sister to a Mediterranean
701 taxon, we hypothesized three biogeographic scenarios for the colonization of the Andes. The first
702 route involves the NALB and North America as a stepwise migration route from Europe ~12–8
703 Ma, whereas the second hypothesis involves a westerly route from Europe through Asia, the
704 Bering Land Bridge, and North America ~12–4 Ma. Both of these scenarios share a second
705 migration from North America to South America over the forming Isthmus of Panama and/or
706 island chains in the mid to late Pliocene ~4.5–3.13 Ma, which gave rise to the *Neobartsia* clade,
707 and high levels of extinction throughout Asia and/or North American. Finally, the third
708 hypothesis involves a long–distance dispersal from the Mediterranean climatic region (Europe
709 and northern Africa) to South America. At this point however, we cannot accept or reject any of
710 the previously described hypotheses. Regardless of the biogeographic route taken, once the
711 South American ancestor reached the Andes, it was able to diversify rapidly in the vacant niches

712 in the páramos. The greater diversification rates in the *Neobartsia* clade help explain the species
713 richness found in the Andes today and support the idea that the "key opportunity" of geographic
714 movement into a new area may trigger high diversification without the necessity of the evolution
715 of morphological key innovations, and this may be especially true when the colonizing ancestral
716 lineage is "pre–adapted" to the new conditions it encounters.

717

718 LITERATURE CITED

719 AGRAWAL, A.A., M. FISHBEIN, R. HALITSCHKE, A.P. HASTINGS, D.L. RABOSKY, AND S.
720 RASMANN. 2009. Evidence for adaptive radiation from a phylogenetic study of plant
721 defenses. *Proceedings of the National Academy of Sciences* 106: 18067–18072.

722 ALFARO, M.E., F. SANTINI, C. BROCK, H. ALAMILLO, A. DORNBURG, D. RABOSKY, G.
723 CARNEVALE, AND L. HARMON. 2009. Nine exceptional radiations plus high turnover explain
724 species diversity in jawed vertebrates. *Proceedings of the National Academy of Sciences*
725 106: 13410.

726 ANTONELLI, A., J.A.A. NYLANDER, C. PERSSON, AND I. SANMARTÍN. 2009. Tracing the impact of
727 the Andean uplift on Neotropical plant evolution. *Proceedings of the National Academy of*
728 *Sciences* 106: 9749–9754.

729 BACON, C.D., W.J. BAKER, AND M.P. SIMMONS. 2012. Miocene Dispersal Drives Island
730 Radiations in the Palm Tribe Trachycarpeae (Arecaceae). *Systematic Biology* 61: 426–442.

731 BALDWIN, B.G. 1992. Phylogenetic Utility of the Internal Transcribed Spacers of Nuclear
732 Ribosomal DNA in Plants: An Example from the Compositae. *Molecular phylogenetics and*
733 *evolution* 1: 3–16.

734 BALDWIN, B.G., AND S. MARKOS. 1998. Phylogenetic Utility of the External Transcribed Spacer
735 (ETS) of 18S–26S rDNA: Congruence of ETS and ITS Trees of Calycadenia (Compositae).
736 *Molecular phylogenetics and evolution* 10: 449–463.

737 BEARDSLEY, P.M., AND R.G. OLMSTEAD. 2002. Redefining Phrymaceae: the placement of
738 Mimulus, tribe Mimuleae, and Phryma. *American Journal of Botany* 89: 1093–1102.

739 BEAULIEU, J.M., D.C. TANK, AND M.J. DONOGHUE. 2013. A Southern Hemisphere origin for
740 campanulid angiosperms, with traces of the break-up of Gondwana. *BMC Evolutionary*
741 *Biology* 13: 80.

742 BELL, C., AND M. DONOGHUE. 2005a. Dating the Dipsacales: comparing models, genes, and
743 evolutionary implications. *American Journal of Botany* 92: 284.

744 BELL, C., AND M. DONOGHUE. 2005b. Phylogeny and biogeography of Valerianaceae
745 (Dipsacales) with special reference to the South American valerians. *Organisms Diversity &*
746 *Evolution* 5: 147–159.

747 BENNETT, J.R., AND S. MATHEWS. 2006. Phylogeny of the parasitic plant family Orobanchaceae
748 inferred from phytochrome A. *American Journal of Botany* 93: 1039–1051.

749 BOLLIGER, M. 1996. Monographie der Gattung Odontites (Scrophulariaceae) sowie der
750 verwandten Gattungen Macrosyringion, Odontitella, Bornmuellerantha und Bartsiella.
751 *Willdenowia* 26: 37–168.

752 BOZLAKER, A., J.M. PROSPERO, M.P. FRASER, AND S. CHELLAM. 2013. Quantifying the
753 contribution of long-range Saharan dust transport on particulate matter concentrations in
754 Houston, Texas, using detailed elemental analysis. *Environmental science & technology* 47:
755 10179–10187.

756 BURNHAM, K.P., AND D.R. ANDERSON. 2002. Model selection and multi-model inference: a
757 practical information-theoretic approach. Second. Springer New York.

758 BURNHAM, R.J., AND A. GRAHAM. 1999. The history of neotropical vegetation: new
759 developments and status. *Annals of the Missouri Botanical Garden*546–589.

760 CHAN, K., AND B. MOORE. 2005. SymmeTREE: whole-tree analysis of differential
761 diversification rates. *Bioinformatics* 21: 1709.

762 COATES, A., L. COLLINS, M. AUBRY, AND W. BERGGREN. 2004. The geology of the Darien,
763 Panama, and the late Miocene-Pliocene collision of the Panama arc with northwestern South
764 America. *Geological Society of America Bulletin* 116: 1327.

765 DAVIS, C.C., C.D. BELL, S. MATHEWS, AND M.J. DONOGHUE. 2002. Laurasian migration explains
766 Gondwanan disjunctions: evidence from Malpighiaceae. *Proceedings of the National*
767 *Academy of Sciences of the United States of America* 99: 6833–6837.

768 DAVIS, C.C., P.W. FRITSCH, C.D. BELL, AND S. MATHEWS. 2004. High-latitude Tertiary
769 migrations of an exclusively tropical clade: evidence from Malpighiaceae. *International*
770 *Journal of Plant Sciences* 165: S107–S121.

771 DENK, T., F. GRIMSSON, AND R. ZETTER. 2010. Episodic migration of oaks to Iceland: Evidence
772 for a North Atlantic "land bridge" in the latest Miocene. *American Journal of Botany* 97:
773 276–287.

774 DENK, T., F. GRÍMSSON, R. ZETTER, AND L.A. SÍMONARSON. 2011. The Biogeographic History of
775 Iceland – The North Atlantic Land Bridge Revisited. *In* Topics in Geobiology, Topics in
776 Geobiology, 647–668. Springer Netherlands, Dordrecht.

777 DONOGHUE, M., AND S. SMITH. 2004. Patterns in the assembly of temperate forests around the
778 Northern Hemisphere. *Philosophical Transactions B* 359: 1633.

779 DONOGHUE, M.J. 2008. A phylogenetic perspective on the distribution of plant diversity.
780 *Proceedings of the National Academy of Sciences of the United States of America* 105:
781 11549–11555.

782 DONOGHUE, M.J., AND M.J. SANDERSON. 2015. Confluence, synnovation, and depauperons in
783 plant diversification. *The New Phytologist*.

784 DOYLE, J.J., AND J.L. DOYLE. 1987. A rapid DNA isolation procedure for small quantities of
785 fresh leaf tissue. *Phytochemical Bulletin* 19: 11–15.

786 DRUMMOND, A., AND A. RAMBAUT. 2007. BEAST: Bayesian evolutionary analysis by sampling
787 trees. *BMC Evolutionary Biology* 7: 214.

788 DRUMMOND, A., S. HO, M. PHILLIPS, AND A. RAMBAUT. 2006. Relaxed phylogenetics and dating
789 with confidence. *PLoS Biology* 4: 699.

790 DRUMMOND, C.S., R.J. EASTWOOD, S.T.S. MIOTTO, AND C.E. HUGHES. 2012. Multiple
791 Continental Radiations and Correlates of Diversification in Lupinus (Leguminosae): Testing
792 for Key Innovation with Incomplete Taxon Sampling. *Systematic Biology* 61: 443–460.

793 EDGAR, R.C. 2004. MUSCLE: multiple sequence alignment with high accuracy and high
794 throughput. *Nucleic Acids Research* 32: 1792–1797.

795 GREGORY-WODZICKI, K. 2000. Uplift history of the Central and Northern Andes: a review.
796 *Geological Society of America Bulletin* 112: 1091.

797 GUINDON, S., AND O. GASCUEL. 2003. A simple, fast, and accurate algorithm to estimate large
798 phylogenies by maximum likelihood. *Systematic Biology* 52: 696–704.

799 GUSSAROVA, G., M. POPP, E. VITEK, AND C. BROCHMANN. 2008. Molecular phylogeny and
800 biogeography of the bipolar Euphrasia (Orobanchaceae): recent radiations in an old genus.
801 *Molecular Phylogenetics and Evolution* 48: 444–460.

802 HO, S., AND M. PHILLIPS. 2009. Accounting for Calibration Uncertainty in Phylogenetic
803 Estimation of Evolutionary Divergence Times. *Systematic Biology* 58: 367–380.

804 HODGES, S.A. 1997. Floral Nectar Spurs and Diversification. *International Journal of Plant*
805 *Sciences* 158: S81–S88.

806 HOPKINS, D.M. 1967. The Bering land bridge. Stanford University Press, Stanfor, CA.

807 HOWE, H.F., AND J. SMALLWOOD. 1982. Ecology of Seed Dispersal. *Annual Review of Ecology*
808 *and Systematics* 13: 201–228.

809 HUGHES, C., AND R. EASTWOOD. 2006. Island radiation on a continental scale: exceptional rates
810 of plant diversification after uplift of the Andes. *Proceedings of the National Academy of*
811 *Sciences* 103: 10334.

812 KIRBY, M.X., AND B. MACFADDEN. 2005. Was southern Central America an archipelago or a
813 peninsula in the middle miocene? A test using land-mammal body size. *Palaeogeography,*
814 *Palaeoclimatology, Palaeoecology* 228: 193–202.

815 MABBERLEY, D.J. 2008. Mabberley's plant-book: a portable dictionary of plants, their
816 classification and uses. 3rd ed. Cambridge, UK. University Press.

817 MAGALLÓN, S., AND M.J. SANDERSON. 2001. Absolute diversification rates in angiosperm clades.
818 *Evolution* 55: 1762–1780.

819 MCNEAL, J.R., J.R. BENNETT, A.D. WOLFE, AND S. MATHEWS. 2013. Phylogeny and origins of
820 holoparasitism in Orobanchaceae. *American Journal of Botany* 100: 971–983.

821 MITTELBACH, G.G., D.W. SCHEMSKE, H.V. CORNELL, A.P. ALLEN, J.M. BROWN, M.B. BUSH,
822 S.P. HARRISON, ET AL. 2007. Evolution and the latitudinal diversity gradient: speciation,
823 extinction and biogeography. *Ecology Letters* 10: 315–331.

824 MOLAU, U. 1990. The genus Bartsia (Scrophulariaceae - Rhinanthoideae). *Opera Botanica* 102:
825 1–100.

826 MOORE, B.R., AND M.J. DONOGHUE. 2007. Correlates of diversification in the plant clade
827 Dipsacales: geographic movement and evolutionary innovations. *The American Naturalist*
828 170 Suppl 2: S28–55.

829 NEE, S., R.M. MAY, AND P.H. HARVEY. 1994. The reconstructed evolutionary process.
830 *Philosophical Transactions of the Royal Society of London. Series B, Biological Sciences*
831 344: 305–311.

832 OLMSTEAD, R.G., C.W. DEPAMPHILIS, A.D. WOLFE, N.D. YOUNG, W.J. ELISONS, AND P.A.
833 REEVES. 2001. Disintegration of the Scrophulariaceae. *American Journal of Botany* 88: 348–
834 361.

835 OSTROM, J.H. 1979. Bird flight: how did it begin? *American Scientist* 67: 46–56.

836 OXELMAN, B., M. LIDÉN, AND D. BERGLUND. 1997. Chloroplast rps16 intron phylogeny of the
837 tribe Sileneae (Caryophyllaceae). *Plant Systematics and Evolution* 206: 393–410.

838 PARADIS, E., J. CLAUDE, AND K. STRIMMER. 2004. APE: Analyses of Phylogenetics and
839 Evolution in R language. *Bioinformatics* 20: 289–290.

840 PENNELL, M.W., J.M. EASTMAN, G.J. SLATER, J.W. BROWN, J.C. UYEDA, R.G. FITZJOHN, M.E.
841 ALFARO, AND A.L.J. HARMON. 2014. geiger v2. 0: an expanded suite of methods for fitting
842 macroevolutionary models to phylogenetic trees. *Bioinformatics*.

843 POSADA, D. 2008. jModelTest: phylogenetic model averaging. *Mol Biol Evol* 25: 1253–1256.

844 PROSPERO, J.M., AND O.L. MAYOL-BRACERO. 2013. Understanding the Transport and Impact of
845 African Dust on the Caribbean Basin. *Bulletin of the American Meteorological Society* 94:

1329–1337.

PROSPERO, J.M., F.X. COLLARD, J. MOLINIÉ, AND A. JEANNOT. 2014. Characterizing the annual cycle of African dust transport to the Caribbean Basin and South America and its impact on the environment and air quality. *Global Biogeochemical Cycles* 29:.

R DEVELOPMENT CORE TEAM. 2013. R: A language and environment for statistical computing. *R Foundation for Statistical Computing, Vienna, Austria. ISBN 3-900051-07-0, URL http://www.R-project.org*.

RABOSKY, D.L., S.C. DONNELLAN, A.L. TALABA, AND I.J. LOVETTE. 2007. Exceptional among-lineage variation in diversification rates during the radiation of Australia's most diverse vertebrate clade. *Proceedings of the Royal Society B: Biological Sciences* 274: 2915–2923.

RAMBAUT, A. 2006. FigTree. *Institute of Evolutionary Biology, University of Edinburgh, Edinburgh, UK. Available at http://tree.bio.ed.ac.uk/software/figtree/*.

RAMBAUT, A. 1996. Se-Al: Sequence alignment editor. *Institute of Evolutionary Biology, University of Edinburgh, Edinburgh, UK. Available at http://tree.bio.ed.ac.uk/software/seal/*.

RAMBAUT, A., AND A.J. DRUMMOND. 2004. Tracer. *University of Edinburgh, Edinburgh, UK. Available at http://tree.bio.ed.ac.uk/software/tracer/*.

REE, R., B. MOORE, C. WEBB, AND M. DONOGHUE. 2005. A likelihood framework for inferring the evolution of geographic range on phylogenetic trees. *Evolution* 59: 2299–2311.

REE, R.H., AND S.A. SMITH. 2008. Maximum Likelihood Inference of Geographic Range Evolution by Dispersal, Local Extinction, and Cladogenesis. *Systematic Biology* 57: 4–14.

RETALLACK, G., AND M. KIRBY. 2007. Middle Miocene global change and paleogeography of Panama. *Palaios* 22: 667–679.

RODRÍGUEZ, F., J.L. OLIVER, A. MARÍN, AND J.R. MEDINA. 1990. The general stochastic model of nucleotide substitution. *Journal of Theoretical Biology* 142: 485–501.

RONQUIST, F., AND J.P. HUELSENBECK. 2003. MrBayes 3: Bayesian phylogenetic inference under mixed models. *Bioinformatics* 19: 1572–1574.

SANDERSON, M.J. 2002. Estimating absolute rates of molecular evolution and divergence times: a penalized likelihood approach. *Molecular Biology and Evolution* 19: 101–109.

SCHEUNERT, A., A. FLEISCHMANN, C. OLANO-MARIN, C. BRÄUCHLER, AND G. HEUBL. 2012. Phylogeny of tribe Rhinantheae (Orobanchaceae) with a focus on biogeography, cytology and re-examination of generic concepts. *Taxon* 61: 1269–1285.

SHIMODAIRA, H. 2002. An approximately unbiased test of phylogenetic tree selection. *Systematic Biology*.

879 SHIMODAIRA, H., AND M. HASEGAWA. 2001. CONSEL: for assessing the confidence of
880 phylogenetic tree selection. *Bioinformatics* 17: 1246–12461247.

881 SHIMODAIRA, H., AND M. HASEGAWA. 1999. Multiple comparisons of log-likelihoods with
882 applications to phylogenetic inference. *Molecular Biology and Evolution* 16: 1114.

883 SIMPSON, B. 1975. Pleistocene changes in the flora of the high tropical Andes. *Paleobiology*273–
884 294.

885 SMITH, S. 2009. Taking into account phylogenetic and divergence-time uncertainty in a
886 parametric biogeographical analysis of the Northern Hemisphere plant clade Caprifolieae.
887 *Journal of Biogeography* 36: 2324–2337.

888 SMITH, S., AND C. DUNN. 2008. Phyutility: a phyloinformatics tool for trees, alignments and
889 molecular data. *Bioinformatics* 24: 715.

890 SMITH, S., AND M. DONOGHUE. 2010. Combining Historical Biogeography with Niche Modeling
891 in the Caprifolium Clade of Lonicera (Caprifoliaceae, Dipsacales). *Systematic Biology*.

892 SMITH, S.A., J.M. BEAULIEU, AND M.J. DONOGHUE. 2009. Mega-phylogeny approach for
893 comparative biology: an alternative to supertree and supermatrix approaches. *BMC*
894 *Evolutionary Biology* 9: 37.

895 STAMATAKIS, A. 2006. RAxML-VI-HPC: maximum likelihood-based phylogenetic analyses
896 with thousands of taxa and mixed models. *Bioinformatics* 22: 2688–2690.

897 STAMATAKIS, A., P. HOOVER, AND J. ROUGEMONT. 2008. A Rapid Bootstrap Algorithm for the
898 RAxML Web Servers. *Systematic Biology* 57: 758–771.

899 SUC, J.P. 1984. Origin and evolution of the Mediterranean vegetation and climate in Europe.
900 *Nature* 307: 429–432.

901 TABERLET, P., L. GIELLY, G. PAUTOU, AND J. BOUVET. 1991. Universal primers for amplification
902 of three non-coding regions of chloroplast DNA. *Plant Molecular Biology* 17: 1105–1109.

903 TANK, D., AND R. OLMSTEAD. 2008. From annuals to perennials: phylogeny of subtribe
904 Castillejinae (Orobanchaceae). *American Journal of Botany* 95: 608–625.

905 TĚŠITEL, J., P. ŘÍHA, Š. SVOBODOVÁ, T. MALINOVÁ, AND M. ŠTECH. 2010. Phylogeny, Life
906 History Evolution and Biogeography of the Rhinanthoid Orobanchaceae. *Folia Geobotanica*
907 45: 347–367.

908 TIFFNEY, B., AND S. MANCHESTER. 2001. The use of geological and paleontological evidence in
909 evaluating plant phylogeographic hypotheses in the Northern Hemisphere Tertiary.
910 *International Journal of Plant Sciences* 162: 3–17.

911 TIFFNEY, B.H. 1985. Perspectives on the Origin of the Floristic Similarity Between Eastern Asia
912 and Eastern North-America. *Journal of the Arnold Arboretum* 66: 73–94.

913 TIFFNEY, B.H. 2008. Phylogeography, Fossils, and Northern Hemisphere Biogeography: The
914 Role of Physiological Uniformitarianism 1. *Annals of the Missouri Botanical Garden* 95:
915 135–143.

916 TRIPP, E.A., AND L.A. MCDADE. 2014. A Rich Fossil Record Yields Calibrated Phylogeny for
917 Acanthaceae (Lamiales) and Evidence for Marked Biases in Timing and Directionality of
918 Intercontinental Disjunctions. *Systematic Biology* 63:660–684:.

919 WIENS, J.J., AND M.J. DONOGHUE. 2004. Historical biogeography, ecology and species richness.
920 *Trends in Ecology & Evolution* 19: 639–644.

921 WOLFE, A., C. RANDLE, L. LIU, AND K. STEINER. 2005. Phylogeny and biogeography of
922 Orobanchaceae. *Folia Geobotanica* 40: 115–134.

923 WOODBURNE, M.O., T.H. RICH, AND M.S. SPRINGER. 2003. The evolution of tribospheny and the
924 antiquity of mammalian clades. *Molecular phylogenetics and evolution* 28: 360–385.

925 YANG, Z. 2006. Computational Molecular Evolution. Oxford University Press.

926 YULE, G.U. 1924. A Mathematical Theory of Evolution, Based on the Conclusions of Dr. J. C.
927 Willis, F.R.S. *Philosophical Transactions of the Royal Society B: Biological Sciences* 213:
928 21–87.

929 ZAGWIN, W.H. 1960. Aspects of the Pliocene and early Pleistocene vegetation and climate in the
930 Netherlands. *Mededelingen Geologische Strichting* 3: 1–78.

931 ZAGWIN, W.H. 1974. The Pliocene-Pleistocene boundary in western and southern Europe.
932 *Boreas* 3: 75–97.

933 ZANNE, A.E., D.C. TANK, W.K. CORNWELL, J.M. EASTMAN, S.A. SMITH, R.G. FITZJOHN, D.J.
934 MCGLINN, ET AL. 2014. Three keys to the radiation of angiosperms into freezing
935 environments. *Nature* 506: 89–92.

936

937

938

Table 1. Taxa and voucher information for plant material from which DNA was extracted. s.n = *sine numero* (without a collecting number). Herbarium abbreviations are as follow: FHO = University of Oxford Herbarium , K = Royal Botanic Gardens Kew , ID, University of Idaho = Stillinger Herbarium , ANDES = Museo de Historia Natural Universidad de los Andes , WTU = University of Washington Herbarium , GH = Harvard University Herbarium , LJU = University of Ljubljana Herbarium , USFS = United States Forest Service , CBFS = University of South Bohemia České Budějovice. GenBank accessions for sequences not generated in this study are also shown.

Species	DNA Voucher/Herbarium	GenBank Accession Number				
		ITS	ETS	trnT-trnL	trnL-trnF	rps16
Bartsia alpina L.	Lampinen s.n/ID	FJ790046	KM408206	KM408239	KM434119	N/A
B. crenoloba Wedd.	Solomon 7152/K	KM408228	KM408185	KM408240	KM434106	KM408308
B. laniflora Benth.	SU-24/ANDES	KM408221	KM408174	KM408242	KM434110	KM408307
B. laticrenata Benth.	Ramsay & Merrow-Smith 771/K	KM408219	KM408178	KM408243	KM434104	N/A
B. melampyroides (Kunth) Benth.	Tank 2005-07/WTU	KM408218	KM408186	KM408245	KM434114	KM408300
B. orthocarpiflora Benth.	Ollgaard 34129/K	KM408216	KM408184	KM408246	KM434111	KM408296
B. pedicularoides Benth.	Jorgenson 1729/K	FJ790047	N/A	FJ790077	N/A	N/A
B. pyricarpa Molau	Tank 2005-36/WTU	KM408226	KM408182	KM408247	KM434102	KM408294
B. ramosa Molau	CG-016/ANDES	KM408229	KM408176	KM408248	KM434108	KM408304
B. santolinifolia (Kunth) Benth.	SU-18/ANDES	KM408220	KM408175	KM408249	KM434109	KM408306
B. sericea Molau	Tank 2005-06/WTU	KM408224	KM408181	KM408250	KM434105	KM408297
B. cf *sericea* Molau	Tank 2005-25/WTU	KM408227	KM408179	KM408251	KM434101	KM408302
B. cf *inaequalis* Benth. *ssp. duripilis* (Edwin) Molau	Tank 2005-29/WTU	KM408225	KM408183	KM408252	KM434107	KM408295
B. stricta (Kunth) Benth.	SU-1b/ANDES	KM408222	KM408177	KM408253	KM434112	KM408305
B. tenuis Molau	Tank 2005-02/WTU	KM408223	KM408180	KM408254	KM434103	KM408299
B. thiantha Diels	RGO 2009-23/WTU	KM408217	KM408187	KM408255	KM434113	KM408303

Bellardia trixago (L.) All.	Bennett s.n/FHO	FJ790063	KM408189	KM408256	KM434100	KM408301
B. viscosa (L.) Fisch. & C.A. Mey	Halse 2249/ID	AY911244	KM408188	KM408273	KM434095	KM408298
Bornmuellerantha aucheri (Boiss.) Rothm.	Oganesian et al. 03-1575/K	KM408237	KM408197	KM408267	KM434116	KM408279
Euphrasia alsa F.Muell.	Zich 220/GH	KM408212	KM408202	KM408257	KM434084	KM408282
E. collina R.Br.	Zich 209/GH	N/A	KM408203	KM408258	KM434086	KM408284
E. mollis (Ledeb.) Wettst.	Mancuso 107/ID	KM408213	N/A	KM408259	KM434082	KM408281
E. regelii Wettst.	Ho 1741/GH	KM408214	N/A	KM408260	KM434085	KM408285
E. stricta D. Wolff ex J.F. Lehm	Musselman 4872/ID	KM408215	N/A	KM408261	KM434098	KM408283
Hedbergia abyssinica (Benth.) Molau var. *abyssinica*	Etuge 3488/K	FJ790061	KM408194	KM408262	KM434120	KM408291
H. abyssinica (Benth.) Molau var. *nykiensis*	Carter et al 2386/K	KM408231	KM408193	KM408263	KM434122	N/A
H. abyssinica (Benth.) Molau var. *petitiana*	Paton s.n/K	KM408230	KM408195	KM408264	KM434123	KM408290
H. decurva (Hochst. ex Benth.) A. Fleischm. & Heubl	Wesche 9/K	N/A	KM408191	KM408241	KM434121	KM408292
H. longiflora ssp. longiflora (Hochst. ex Benth.) A. Fleischm. & Heubl	Kisalye van Heist 109/K	KM408232	KM408192	KM408244	KM434099	KM408286
Lathraea squamaria L.	Frajman s.n/LJU	FJ790044	KM408204	EU264174	KM434087	KM408309
Melampyrum carstiense Fritsch	Krajsek s.n/LJU	GU445314	N/A	EU264177	KM434088	KM408315
M. lineare Lam.	Bjork 6465/ID	KM408208	KM408207	KM408265	KM434096	KM408316
M. sylvaticum L.	Krajsek s.n/LJU	EU624134	N/A	KM408266	KM434089	KM408314
Odontites corsicus (Loisel.) G. Don	J. Stefani/ID	KM408238	KM408200	KM408268	KM434117	N/A
O. linkii Heldr. & Sart. ex Boiss. *ssp cyprius*	Ferguson 4537/K	KM408234	KM408196	KM408269	KM434083	KM408288
O. maroccanus Bolliger	Gattefose s.n/K	KM408233	KM408198	KM408270	KM434097	N/A
O. vulcanicus Bolliger	Bolliger & Moser O-M3/K	KM408235	KM408199	KM408271	KM434115	KM408289
O. vulgaris Moench	Kharkevich s.n/K	KM408236	KM408201	KM408272	KM434118	KM408287
Rhinanthus crista-galli L.	Bjork 6656/ID	KM408210	N/A	KM408274	KM434091	KM408313
R. freynii (A.Kern. ex Sterneck) Fiori	Mathews 04-05	GU445319	KM408205	KM408275	KM434092	KM408310
R. kyrollae Chabert	Stickney 1236/USFS	KM408209	N/A	KM408276	KM434090	KM408312
R. serotinus (Schönh.) Oborny	Musselman 4871/ID	KM408211	N/A	KM408277	KM434093	KM408311
Rhynchocorys elephas Griseb.	Tesitel 5044/CBFS	FJ790055	N/A	FJ790085	N/A	N/A
R. kurdica Nábělek	Tesitel 5042/CBFS	FJ790037	N/A	FJ790067	N/A	N/A
R. maxima Richter	Tesitel 5040/CBFS	FJ790037	N/A	FJ790067	N/A	N/A
R. odontophylla R.B.Burbidge & I.Richardson	Tesitel 5038/CBFS	FJ790034	N/A	FJ790064	N/A	N/A
R. orientalis Benth.	Tesitel 5039/CBFS	FJ790035	N/A	FJ790065	N/A	N/A

R. stricta Albov	Tesitel 5047/ CBFS	FJ790057	N/A	FJ790087	N/A	N/A
Tozzia alpina L.	Mathews 04-04	AY911258	KM408190	KM408278	KM434094	KM408280

Table 2. Results for the Approximately Unbiased (AU) and the Shimodaira–Hasegawa (SH) tests at $p < 0.05$ for different constrained relationships. Log likelihood scores for the original analysis are given, as well as the difference in log likelihood between the original and the constraint topology (∂). Values in bold are significant with 95% confidence.

nrDNA analysis constraint compared to clades from the cpDNA analysis	ln likelihood	∂	AU	SH
Unconstrained nrDNA analysis	–8445.56			
Tozzia + *Hedbergia*	–8449.04	3.48	0.166	0.186
H. decurva + *H. abyssinica* var. *nykiensis*	–8464.51	18.95	**0.004**	**0.026**
Odontites + *Bellardia*	–8456.43	10.87	0.141	0.131

cpDNA analysis constraint compared to clades from the nrDNA analysis				
Unconstrained cpDNA analysis	–10044.47			
Tozzia + *Bellardia*	–10064.45	19.98	**0.001**	**0.017**
H. decurva + *H. longiflora* ssp. *longiflora*	–10053.20	8.73	0.07	0.101
Odontites + *Euphrasia*	–10071.61	27.14	**0.0004**	**0.008**

Table 3. Divergence time estimates for the main clades, with each node representing the most recent common ancestor (mrca) of the taxa mentioned. The first value was obtained by calibrating the node of divergence of *Melampyrum* from its sister clade. The calibration point had a prior with lognormal distribution, offset 25 Myr, mean of 0.9, and standard deviation of 0.8, using the results of Wolfe et al. (2005), but incorporating considerable temporal uncertainty. The second value corresponds to an additional analysis where the uplift of the Andes was used as the calibration point of the node of divergence for S. Am. *Bellardia*. This last calibration had a prior with a lognormal distribution, offset of 1.7 Myr, mean of 0.2, and standard deviation of 0.6. Median age estimates as well as the 95% highest posterior density (HPD) are shown for both analyses. In addition, the composite Akaike weights (w_i) from our biogeographic analyses are shown for the 'expert based' coding of current geographic distributions with the following abbreviations: A (Africa), EU (Europe), EUR (Eurasia), ENA (Eastern North America), SAM (South America). Evidence ratio is presented for the most supported geographic reconstruction.

Node (mrca)	Median Age (Ma)	95% HPD (Ma)	w_i	Evidence Ratio
Root	30.65 / 30.98	25.55–38.83 / 29.13–35.96	EU 0.31	1.82
Melampyrum	14.70 / 15.02	7.41–24.89 / 7.14–24.32	EU 0.18	1.8
Lathraea–Bellardia	27.01 / 27.38	25.19–31.64 / 20.87–33.57	EU 0.53	3.8
Rhynchocorys–Lathraea	20.53 / 20.33	15.18–26.27 / 13.97–26.88	EU 0.58	2.4
Rhinanthus–Lathraea	16.66 / 16.49	10.78–22.64 / 10.37–23.14	EU 0.53	2.2
Rhynchocorys	11.65 / 11.57	7.13–17.43 / 6.69–17.45	EU 0.49	2.13
Bartsia alpina–Bellardia	22.62 / 22.33	17.49–28.07 / 16.23–28.36	EU 0.44	1.69
Euphrasia–Bellardia	19.25 / 19.02	14.35–24.23 / 13.72–24.60	EU+EUR 0.43	1.95
Euphrasia	6.66 / 6.57	3.53–10.31 / 3.60–10.38	EUR 1.0	–
Tozzia–Bellardia	16.62 / 16.42	12.23–21.75 / 11.61–21.48	EU 0.53	1.76
Tozzia–Hedbergia	13.64 / 13.51	8.78–18.70 / 8.69–18.75	A+EU 0.94	23.5
H. longiflora–H. decurva	6.94 / 6.90	3.67–10.93 / 3.60–10.96	A 0.99	247.5
Odontites–Bellardia	14.61 / 14.39	10.13 –19.26 / 9.93–19.19	EU 0.80	8.88
Odontites	9.38 / 9.29	6.22–13.02 / 5.94–13.29	EU 1.0	–
Bellardia trixago–Neobartsia clade	8.73 / 8.48	5.12–12.76 / 4.95–12.48	EU+SAM 0.26 EU 0.18 EU+EUR+SAM 0.16	1.44 1.13 –
Bellardia viscosa–Neobartsia clade	7.39 / 7.16	4.21–11.24 / 4.03–10.84	EU+SAM 0.53 EU+EUR+SAM 0.35	1.51 11.66
Neobartsia clade	2.59 / 2.63	1.51–4.08 / 1.97–3.58	SAM 1.0	–

Table 4. The composite Akaike weights (w_i) are shown for our three different coding scenarios: conservative, expert based, and species specific. Abbreviations are as follow: A (Africa), EU (Europe), EUR (Eurasia), ENA (Eastern North America), SAM (South America). Evidence ratio is presented for the most supported geographic reconstruction.

Coding Scheme	*Conservative*		*Expert based*		*Species specific*	
Node (mrca)	w_i	Evidence Ratio	w_i	Evidence Ratio	w_i	Evidence Ratio
Root	EU 0.52	3.71	EU 0.31	1.82	EU+ENA 0.40	1.05
Melampyrum	EU 0.25	3.57	EU 0.18	1.8	EU+ENA 0.93	4.65
Lathraea–Bellardia	EU 0.81	11.6	EU 0.53	3.8	EU 0.76	8.4
Rhynchocorys–Lathraea	EU 0.73	8.11	EU 0.58	2.4	EU 0.92	13.14
Rhinanthus–Lathraea	EU 0.67	6.1	EU 0.53	2.2	EU 0.96	13.7
Rhynchocorys	EU 0.62	5.16	EU 0.49	2.13	EU 0.70	2.59
Bartsia alpina–Bellardia	EU 0.84	16.8	EU 0.44	1.69	EU 0.59	3.10
Euphrasia–Bellardia	EU 0.80	26.6	EU+EUR 0.43	1.95	EU+EUR 0.40	1.81
Euphrasia	EU 0.26	2.88	EUR 1.0	–	EUR 1.0	–
Tozzia–Bellardia	EU 0.74	5.28	EU 0.53	1.76	EU 0.53	1.96
Tozzia–Hedbergia	A+EU 0.90	11.25	A+EU 0.94	23.5	A+EU 0.91	15.16
Hedbergia	A 0.98	122.5	A 0.99	247.5	A 0.98	81.66
Odontites–Bellardia	EU 0.79	26.03	EU 0.80	8.88	EU 0.76	7.6
Odontites	EU 0.74	6.16	EU 1.0	–	EU 0.93	15.5
B. trixago–Neobartsia	EU+SAM 0.21	1.31	EU+SAM 0.26	1.44	EU+SAM 0.24	1.33
clade	EU 0.16	1.45	EU 0.18	1.13	EU 0.18	1.06
	EU+EUR+SAM 0.11	–	EU+EUR+SAM 0.16	–	EU+EUR+SAM 0.17	–
B. viscosa–Neobartsia	EU+SAM 0.48	1.77	EU+SAM 0.53	1.51	EU+SAM 0.49	1.29
clade	EU+EUR+SAM 0.27	6.75	EU+EUR+SAM 0.35	11.66	EU+EUR+SAM 0.38	12.66
Neobartsia clade	SAM 1.0	–	SAM 1.0	–	SAM 1.0	–

Table 5. Results from our diversification rate analyses using MEDUSA and SymmeTREE over a posterior distribution of trees. The shifts were found at the nodes subtending the taxa specified in the first column, followed by the frequency of that shift in the posterior distribution of trees, the net diversification rate (*r*) for the maximum clade credibility tree (mcc), and the mean, median, minimum (min), maximum (max), and standard deviation (sd) summarized across 1,000 trees from the posterior distribution. In the results for SymmeTREE, two different significance values (α) were examined, $\alpha < 0.05$, and $\alpha < 0.10$.

Node	Freq. shift	*r* mcc	r mean	r median	r min.	r max.	r sd
MEDUSA							
Bartsia alpina	1.17	0	–0.04	–0.15	–0.32	0.33	0.18
Tozzia–Hedbergia	0.75	0.05	–0.06	0.00	–0.36	0.73	0.14
Neobartsia clade	0.40	0.79	0.40	0.38	0.15	1.03	0.13
Clade sister to *Bartsia alpina*	0.32	n/a	0.09	0.12	–0.18	0.26	0.07
Rhinanthus –Lathraea	0.12	n/a	0.17	0.16	0.12	0.28	0.03
Core *Rhinantheae*	0.07	n/a	0.11	0.12	–0.11	0.47	0.07

SymmeTREE	**Freq. shift at p < 0.05**	**Freq. shift p < 0.10**
Bartsia alpina	1.00	1.00
Tozzia–Hedbergia	0.00	0.93
Neobartsia clade	0.14	0.48

Figure 1

Majority rule consensus tree (excluding burn–in trees) with mean branch lengths from the partitioned Bayesian analysis of the combined dataset. Branch lengths are proportional to the number of substitutions per site as measured by the scale bar. Values above the branches represent Bayesian posterior probabilities (PP) and maximum likelihood bootstrap support (BS). Major clades are summarized following species names with the current species diversity in parenthesis.

Figure 2

Majority rule consensus tree (excluding burn–in trees) with mean branch lengths from the partitioned Bayesian analysis of the a) nuclear ribosomal (nr) DNA and b) the chloroplast (cp) DNA datasets. Branch lengths are proportional to the number of substitutions per site as measured by the scale bar. Values above the branches represent Bayesian posterior probabilities (PP) and maximum likelihood bootstrap support (BS).

Figure 3

Topology obtained after combining and annotating five independent BEAST analyses. The calibration point was set at the node where all genera are included except for *Melampyrum*. The calibration had a prior with a lognormal distribution, offset 25 Ma, a mean of 0.9, and a standard deviation of 0.8 following dates by by Wolfe et al. (2005). Time in millions of years ago (Ma) is represented by the scale below the tree. Current distributions of the species are color–coded after the species names. The current distributions are plotted on a map below the species names and correspond to blue for Eurasia, red for Europe, yellow for Africa, black for northeastern North

America, and green for South America. The most supported ancestral range reconstructions obtained from a Lagrange analysis, are plotted on the tree with color rectangles or circles with numbers that represent different biogeographic hypotheses. Ancestral range reconstruction scenarios are plotted on five different maps on the left of the figure, each with a number that distinguishes it. Composite Akaike weights (w_i) are plotted in the form of histograms for nodes where the reconstruction had competing hypotheses. Two possible routes of migration, one including the North Atlantic Land Bridge (NALB) and one including the Bering Strait, are shown on maps 5 and 6.

142 Figure 1

143

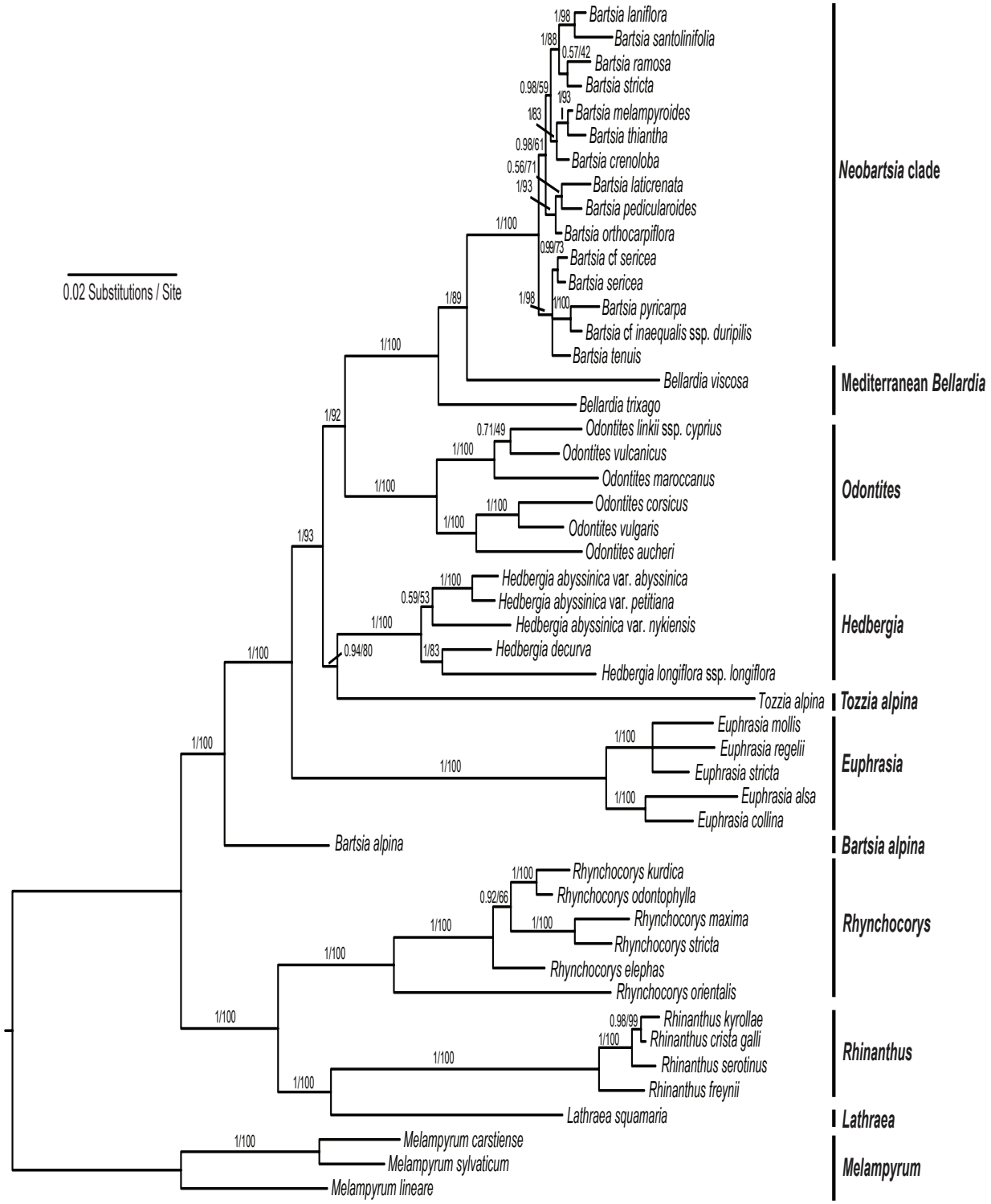

144

145 Figure 2

146

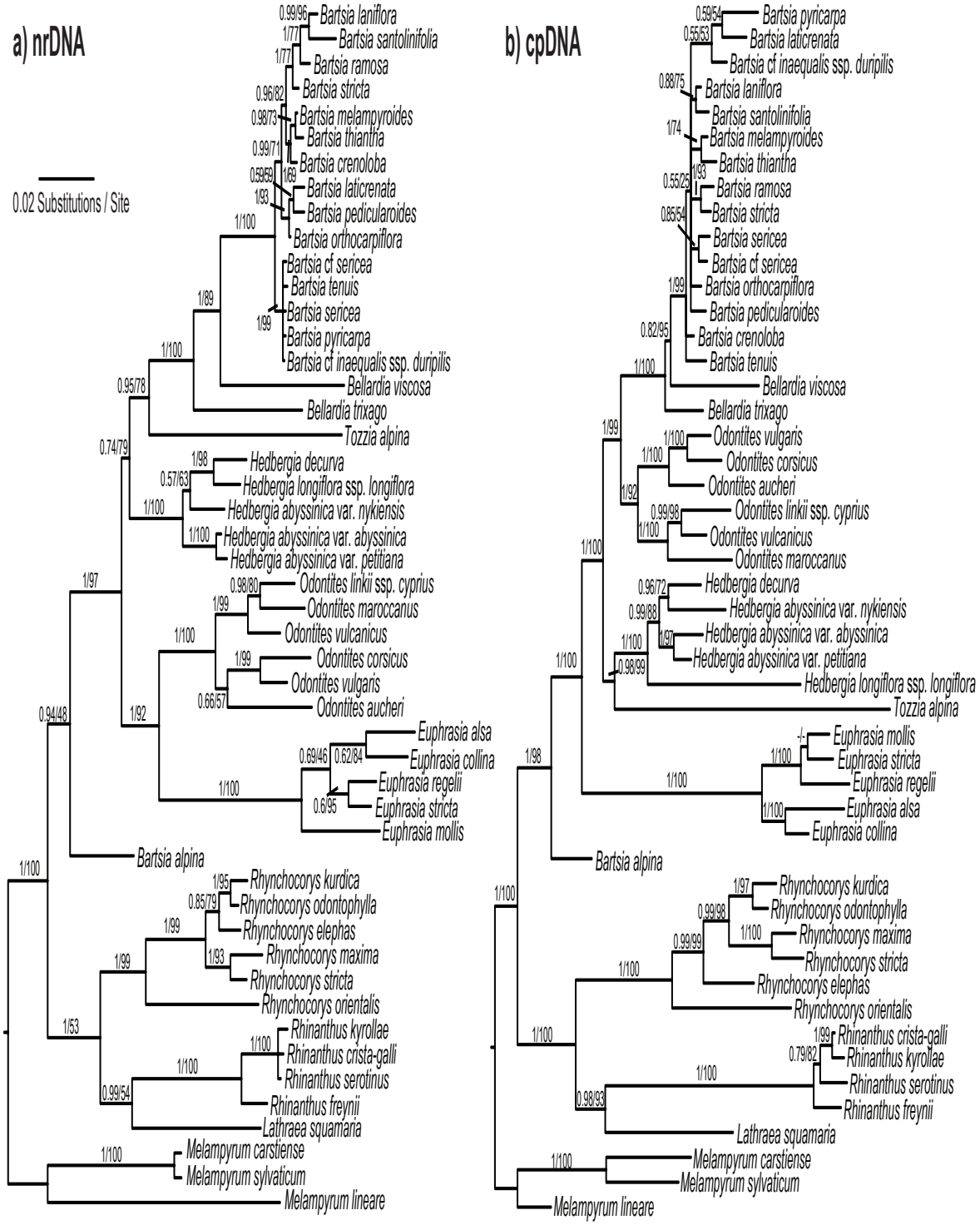

147

148 Figure 3

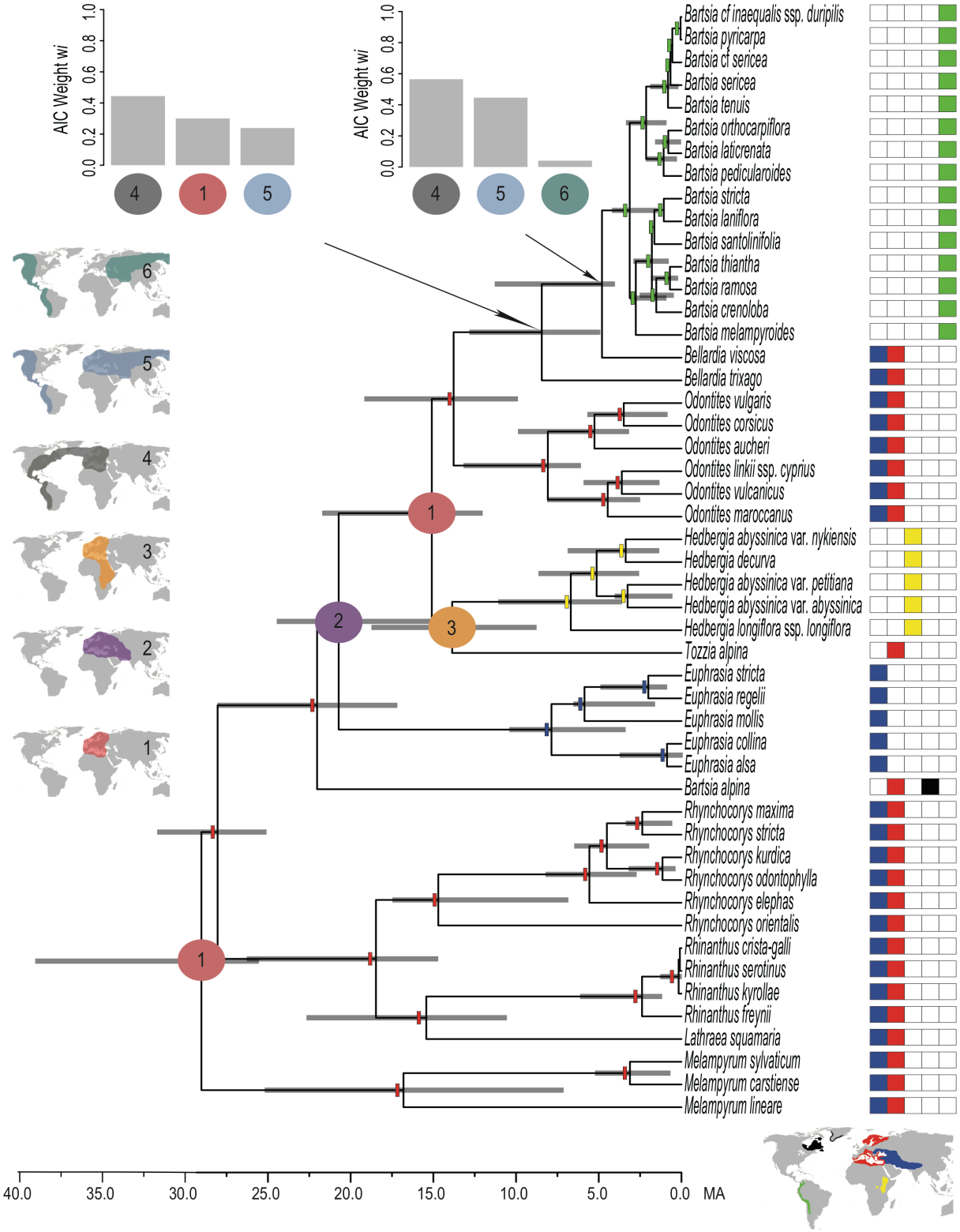

149